Linking compound weather extremes to Mediterranean cyclones, fronts and air streams

Alice Portal[1], Shira Raveh-Rubin[2], Jennifer L Catto[3], Yonatan Givon[2], and Olivia Martius[1]

[1]Institute of Geography, Oeschger Centre for Climate Change Research, University of Bern, Bern, Switzerland
[2]Department of Earth and Planetary Sciences, Weizmann Institute of Science, Rehovot, Israel
[3]Department of Mathematics and Statistics, University of Exeter, Exeter, United Kingdom

Correspondence: Alice Portal (alice.portal@unibe.ch)

Abstract. Mediterranean cyclones are the primary driver of many types of surface weather extremes in the Mediterranean region, the association with extreme rainfall being the most established. The large-scale characteristics of a Mediterranean cyclone, the properties of the associated airflows and temperature fronts, the interaction with the Mediterranean Sea and with the topography around the basin, and the season of occurrence, all contribute in determining its surface impacts. Here, we take these factors into account to interpret the statistical links between Mediterranean cyclones and compound extremes of two types, namely co-occurring rain–wind and wave–wind extremes. Compound extremes are attributed to a cyclone if they fall within a specially defined *Mediterranean cyclone impact area*. Our results show that the majority of Mediterranean rain–wind and wave–wind extremes occur in the neighbourhood of a Mediterranean cyclone, with local peaks exceeding 80%. The fraction of compounds happening within a cyclone's impact area is highest when considering transition seasons, and for rain–wind events compared with wave–wind events. Winter cyclones, matching with the peak occurrence of large and distinctively baroclinic cyclones, are associated with the highest compound frequency. A novel deconstruction of cyclones' impact areas based on the presence of objectively-identified air streams and fronts reveals a high incidence of both types of compound extremes below warm conveyor belt ascent regions, and of wave–wind extremes below regions of dry intrusion outflow.

1 Introduction

In November 2011 a Mediterranean cyclone named Rolf struck the western Mediterranean basin causing fatalities and damage in the Balearic Islands, Southern France, Corsica and Northern Italy. The cyclone formed on November 5th through the interaction of a strong eastward-propagating front with the Pyrenees; it then remained stationary south of the French coast for approximately four days, where it developed tropical like characteristics (see details in Dafis et al., 2018; Gutiérrez-Fernández et al., 2024), before making landfall in south-eastern France and dissipating on November 10th. The stationarity and intensity of Rolf resulted in persistent torrential rainfall, strong winds and high waves, leading to floods, landslides and treefalls (The Washington Post, 2011; DWD, 2011). Major impacts, ranging from house evacuations, traffic disruptions and blackouts to costly infrastructural damage in the public and private sectors, affected "Var département" in France and "regione Liguria" in Italy, extending to other adjacent areas (Impact Forecasting LLC, 2011). This is only one example of a high-impact compound extreme event brought by the passage of a Mediterranean cyclone.

The compounding of extreme events (referred in the following as "compound extremes" or simply "compounds") constitutes a higher societal and economic risk compared with single extreme events (Zscheischler et al., 2018; Seneviratne et al., 2012; Ridder et al., 2020; Zscheischler et al., 2020). In this work we focus on the co-occurrence of meteorological hazards, specifically of extreme rain[1] and wind, and extreme wave height and wind, because of the potential impacts of these weather conditions in the European region (Ridder et al., 2020; De Luca et al., 2020).

Severe weather in the mid latitudes is often associated with the presence of extratropical cyclones (e.g., Jansa et al., 2001; Nissen et al., 2010). Coherent air streams and surface impacts are arranged around the storm's low-pressure centre by the anticyclonic circulation, according to a conceptual extratropical-cyclone model (e.g., Carlson, 1980; Schultz et al., 2019, and references therein). In the eastern warm sector, warm moist air, namely the *warm conveyor belt*, ascends northward and around the cyclone centre, producing intense precipitation (Madonna et al., 2014). The *cold front*, separating the warm and cold sector of the cyclone, trails to the south of the storm and produces pre-frontal convective activity (Catto and Pfahl, 2013). In satellite imagery the combination of warm conveyor belt and cold front form a synoptic-scale comma shaped cloud structure wrapping around the cyclone from the south east. In the western cold sector, anomalously dry and cold airflows descending from the north generate a predominantly cloud-free region, characterised by isolated convection forming cumulus-type clouds. Specifically, *dry intrusions* transport cold and dry air from the upper troposphere and, when interacting with the warmer boundary layer, may generate strong surface wind gusts and low-level instability to the south of the cyclone (Raveh-Rubin, 2017).

Mediterranean cyclones, generally shorter-lived and smaller than their Atlantic equivalents (e.g. Campins et al., 2011; Lionello et al., 2016), share the aforementioned dynamical features (Flaounas et al., 2022, 2015), although interactions with regional topography may modify the distribution of air streams and surface impacts. A recent classification of Mediterranean cyclones based on their large scale dynamics unveils differences in terms of life-cycle characteristics, spatio-temporal occurrence and associated meteorological hazards (Givon et al., 2024a), and proves useful for understanding which types of cyclones are most prone to inducing compound extremes.

The passage of cyclones around the Mediterranean basin is statistically well-linked to regional (extreme) weather conditions in terms of precipitation (Pfahl and Wernli, 2012; Jansa et al., 2001; Pfahl, 2014) and wind (Pfahl, 2014; Nissen et al., 2010; Dowdy and Catto, 2017). The connection with rain–wind extremes has received less attention at this regional scale (for works on larger domains see Owen et al., 2021; Ridder et al., 2020; Catto and Dowdy, 2021). Recent studies on Mediterranean rain–wind extremes consider a small sample of large-scale events (Raveh-Rubin and Wernli, 2015) or take a Lagrangian cyclone-centred perspective (Rousseau-Rizzi et al., 2023). The concomitant occurrence of high waves and strong winds within the Mediterranean Sea has been hardly analysed, in spite of the considerable impacts, e.g., infrastructural damage along the coast, interruption of vessel traffic, or ship accidents (Cavaleri et al., 2012; Bertotti and Cavaleri, 2008; Zhang and Li, 2017), and of its societal relevance when considering the many people crossing the Mediterranean on poor quality boats.

In this work, we perform a benchmark analysis of the distributions of compound extremes (rain–wind and wave–wind, Section 2.1) and of their association with Mediterranean cyclone tracks (Section 2.2) against existing literature. Our work extends previous studies by using the latest datasets to examine a range of yet unexplored settings and questions. In particular,

---

[1]The term rain is here generalised to indicate precipitation

we analyse mutual dependencies between compound extremes and Mediterranean cyclones to tackle the following research questions:

1. Does the presence of a cyclone impact the frequency of compound extremes? What proportion of compounds is associated with a nearby cyclone? (Sections 4, 4.1, 4.2)

2. Which amongst cyclone cold fronts, dry intrusions or warm conveyor belts (referred to collectively as *dynamical features*) is the most important for compound extremes? (Sections 4.1, 4.2)

3. Extending the work by Givon et al. (2024a), what types of cyclones are locally relevant for the occurrence of compound extremes? (Section 4.3)

While exploring the statistics of compounds and cyclones from a (geographical) Eulerian perspective, we put equivalent emphasis on winter and on transition seasons (autumn, spring) because of severe cyclone-related weather conditions occurring at such times.

An additional yet fundamental methodological question concerns the attribution of weather events to Mediterranean cyclones. This has been done in Flaounas et al. (2018) for the case of intense regional rainfall, but their method is too restrictive for identifying extreme surface winds and waves, often happening at some distance from the storm centre (Nissen et al., 2010; Pfahl, 2014; Raveh-Rubin and Wernli, 2016). Alternative reference approaches are designed for extratropical cyclones in general, which spend most of their lifecycle over open ocean (e.g., Catto and Dowdy, 2021). Here we propose an alternative definition for a *Mediterranean cyclone impact area* that takes into account the type of compound, the peculiarity of the geographic setting and the synoptic air streams and fronts developing around the system (Section 3).

2   Data and methods

2.1   Compound extremes

Uni-variate extremes of 6 h cumulative precipitation (rain), maximum 10 m wind gust (wind), and maximum significant swell and wave height (wave) are identified in the ERA5 reanalysis dataset (Hersbach et al., 2020) from January 1980 to December 2019. The data have a temporal frequency of 6 hours, with accumulations or maxima computed for each 6 h time interval centred around hours 00, 06, 12, 18 UTC. A horizontal resolution of $0.5°$ suffices for the identification of surface extremes with scales from the order of 100 km, as those typically induced by synoptic-scale weather systems, but is unable to capture small-scale (convective-driven) extremes. Grid-point values exceeding the local 98th year-round percentile (other percentiles were tested) and a minimum threshold of 2 mm for rain, 10 ms^{-1} for wind and 2 m for waves constitute our sample of uni-variate extremes (see maps of thresholds in Fig. SM1[2]); these are classified as rain–wind or wave–wind compound extremes when occurring at the same time step and grid point.

---

[2]SM figure label refers to the Supplementary Material document

We adopt year-round thresholds for the identification of extremes to obtain consistent and potentially impactful events across seasons, with minimum thresholds intended for neglecting those occurrences which, despite belonging to the upper quantile, are very weak in intensity (e.g., rainfall over the Sahara, see Fig. SM1). Weather extremes from the upper two percentiles, although allowing for a limited detection of summer compounds of both types, provide an adequate sampling of compounds during the other seasons. The selection comprises extremes with varied impact potential: while the effects of extreme 6 h rain depend on its accumulation over hourly to seasonal time spans (e.g., Guzzetti et al., 2008; Froidevaux et al., 2015; Kilsdonk et al., 2022), wind events of this type are damage-relevant (Klawa and Ulbrich, 2003). Allthemore, it is worth bearing in mind that, although not all statistically extreme meteorological conditions have serious societal or environmental consequences, extremes that are *per se* moderate occasionally combine to produce severe impacts (Seneviratne et al., 2012).

For estimating rainfall we use ERA5 total precipitation, corresponding to the sum of the large-scale and convective precipitation generated by the ECMWF Integrated Forecasting System (IFS). Since the IFS grid (∼30 km spacing in the horizontal) does not resolve convective processes, these are parametrised; note that convection can be relevant for the (concomitant) occurrence of small-scale rain, wind and wave extremes. Lavers et al. (2022) visually compare ERA5 patterns with four observed impactful rainfall extremes and show a satisfactory performance of the reanalysis, notwithstanding a negative bias in representing the highest precipitation totals. The temporal correspondence between observed and ERA5 intense precipitation events is estimated to be around 40-50% by Rivoire et al. (2021). Owen et al. (2021) analyse the geographical and temporal distribution of compound rain–wind extremes and report a high consistency between ERA5 and observed datasets. The simulation of wind gust and waves in ERA5 has improved with respect to ERA-Interim (Hersbach et al., 2020), although negative wind gust biases are measured inland and over orography because of the incorrect representation of wind channeling (see Minola et al. (2020); Obermann-Hellhund (2022) and ECMWF user guide [3]) and negative wave biases are reported, especially around coastal areas (Fanti et al., 2023).

2.2 Mediterranean cyclones

We consider cyclones over the Mediterranean region in the period 1980–2019. The cyclone tracks are a result of the efforts of the MedCyclones COST Action [4] to produce a reference dataset of cyclone intensity and position (i.e., the value and location of the SLP minimum) within the Mediterranean region. The composite tracking approach described in Flaounas et al. (2023) combines ten different cyclone detection and tracking methods applied to the ERA5 reanalysis (Hersbach et al., 2020) to identify cyclones spending at least 24 h in a broad Mediterranean domain (20°–50° N and 20° W–45° E). Although the tracks are computed on the original ERA5 temporal and spatial resolution, in this study, for consistency with the compound data described in Section 2.1, we interpolate the position onto a 0.5° horizontal grid and select the time steps coinciding with the hours 00, 06, 12, 18 UTC.

As in recent articles using the Flaounas et al. (2023) cyclone dataset (see Givon et al., 2024a; Rousseau-Rizzi et al., 2023), we select the tracks with confidence-level of 5, i.e., those satisfying an agreement among a minimum of five detection methods

---

[3]https://confluence.ecmwf.int/display/CKB/Windstorm+footprints%3A+Product+User+Guide

[4]See website at https://medcyclones.eu/

120   for at least 12 h in the cyclone's lifetime. The selection yields 3043 cyclones from 1980 to 2019, excluding many shallow heat lows occurring in summer or in the transition seasons (Givon et al., 2024a).

2.2.1 Cyclone clusters

A clustering of the aforementioned Mediterranean cyclones based on their upper-level PV characteristics is performed by Givon et al. (2024a). They obtain nine cyclone classes (identified by numbers), which differ by construction in terms of upper-level
125   dynamics and synoptic-scale drivers, but also reveal a dominant seasonality and spatial distribution, together with distinctive tropospheric characteristics and surface impacts (see Table 1). Clusters 1, 2 and 4 are winter baroclinic cyclones (stage-A and -B lee lows and cyclones developing from Rossby wave breaking, respectively), clusters 5 and 8, peaking in the transition seasons, correspond to anticyclonic and cyclonic wave breaking, while clusters 3 and 7, showing maximum occurrence in spring, are associated with long wave cut-off lows and daughter lows, respectively; clusters 6 and 9, often land based and
130   displaying a shallow low-level structure, are summer lows (Sharav heat low and short-wave cut-off low, respectively). For more details refer to Givon et al. (2024a) and Rousseau-Rizzi et al. (2023).

2.3 Dynamical features

Mediterranean cyclones, as extratropical cyclones in general, are circulation anomalies which displace air masses and create strong temperature gradients (Flaounas et al., 2022; Carlson, 1980). In this work we consider three types of air streams and
135   fronts typical of extratropical cyclones, namely warm conveyor belts (WCBs), dry intrusions (DIs) and cold fronts (CFs), and we analyse their links to compound extremes. A schematic of their organisation around Mediterranean cyclones and of the related surface impacts is provided in Fig. 17 of Raveh-Rubin and Wernli (2016).

We use existing datasets of objectively identified dynamical features to label boolean feature masks, as in the following:

- WCB masks where the WCB inflow and ascent trajectory density is greater than zero. Lagrangian WCB trajectories are
140   identified in the ERA5 reanalysis based on an ascent of at least 600 hPa within 48 hours and on the presence of a nearby extratropical cyclone (Madonna et al., 2014; Heitmann et al., 2023; Wernli and Davies, 1997; Sprenger et al., 2017); the areas of low-level inflow (up to 800 hPa) and mid-level ascent (up to 400 hPa) are taken into account. Because Heitmann et al. (2023)'s global cyclone tracks include a different set of systems and because they use a different WCB–cyclone attribution method, in this work WCB objects are not strictly associated with a Mediterranean cyclone track;

145   - DI masks where the trajectory density of DI outflow[5] is greater than zero. DI-outflow trajectories, identified in ERA5 based on a descent of at least 400 hPa within 48 h (Raveh-Rubin, 2017), are selected in the lower troposphere (up to 700 hPa) as in Catto and Raveh-Rubin (2019);

- CF masks around CF lines. CF lines are detected in ERA5 reanalysis following Hewson (1998) and Sansom and Catto (2022) and are extended by a 2.5° distance to obtain a 2-dimensional object around each front as in Catto and Pfahl
150   (2013).

---

[5]The original DI dataset is smoothed using 2d convolution on a 4-by-4 symmetric kernel, in order to connect fragmented masks into single DI objects.

Feature masks of WCB inflow and ascent, DI outflow and CF area correspond to connected objects[6] satisfying the conditions above; examples are shown in Fig. 1(b). Furthermore, based on the "impact area criteria" described in Section 3, each feature mask is attributed - or not - to any of the co-occurring Mediterranean cyclones; cyclone-less features are labeled as "stray".

2.4 Notation

155 We express the percentage frequency of an event e as $p(e) = 100 \cdot n(e)/N\%$, where $n(e)$ is the number of events and N is the total number of time steps. The percentage frequency of e conditional on event f is represented by $p(e\,|f) = 100 \cdot n(e \wedge f)/n(f)\%$, where $\wedge$ indicates co-occurrence of two events ($\vee$ indicates occurrence of at least one of the two events).

3 An *impact area* for Mediterranean cyclones

The *impact area* is the region around a cyclone centre within which an event (e.g., a compound extreme) is associated to the
160 presence of that cyclone. In the literature on extratropical cyclones many possibilities are explored:

- geometric definitions using a specific radius around the cyclone centre (e.g., a 1000 km radius in Owen et al. (2021), a 1100 km radius in Utsumi et al. (2016), or variable radii in Hepworth et al. (2022));

- dynamical definitions based on closed SLP contours, as in Pfahl and Wernli (2012); Papritz et al. (2014); Dowdy and Catto (2017);

165 - in some cases, the contribution of dynamical features related to the presence of the cyclones is also taken into account (e.g., cold fronts in Papritz et al., 2014), or advocated for (Pfahl and Wernli, 2012).

Mediterranean cyclones are on average weaker, smaller and shorter-lived than their North-Atlantic equivalents (Trigo et al., 1999; Trigo, 2006; Čampa and Wernli, 2012; Campins et al., 2011). However, a Mediterranean cyclone's impact area must account for the interactions of the induced atmospheric flow with coastal boundaries and orographic features, since these
170 modify the spatial distribution of the surface impacts (Pfahl, 2014; Houze Jr, 2012; Obermann-Hellhund, 2022; Owen et al., 2021; Flaounas et al., 2019) compared with a conceptual airflow model of an extratropical cyclone over the ocean (Carlson, 1980; Wernli and Davies, 1997; Schultz, 2001). The position of a cyclone centre relative to the coast and to the Mediterranean sea, the main source of moisture, also determines the character of the impacts (Jansa et al., 2001; Pfahl, 2014).

Reconciling the above aspects, and based on the observation of the synoptic maps and the extreme impacts of the eighty-six
175 Mediterranean cyclone tracks occurring in year 1980[7], we define an impact area for Mediterranean cyclones (labeled IA01) as a fixed *central area*, a circle of 1000 km radius from the cyclone centre[8], eventually extended by the feature masks satisfying the conditions below:

---

[6]Regions of unit-valued grid points connected via a structuring element [[111][111][111]] which allows for diagonal connections.

[7]Maps available at https://boris.unibe.ch/id/eprint/192315

[8]A fixed-radius area is here preferred to a SLP-based dynamical area because of Mediterranean orography inducing uncertainties in the SLP field (Flaounas et al., 2015).
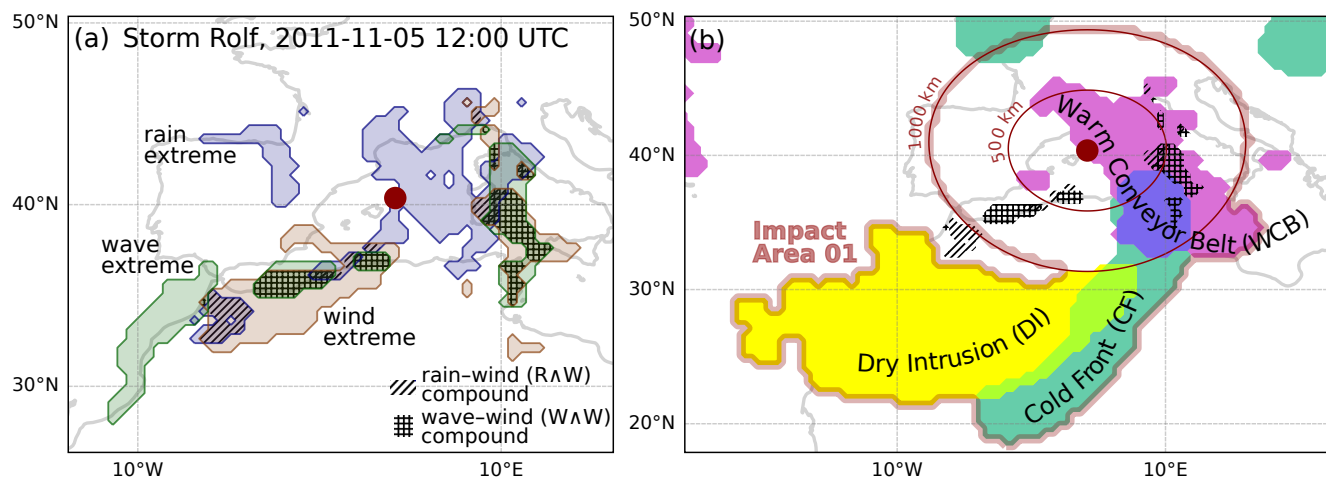
Figure 1. The dark red dot indicates Cyclone Rolf's centre at 12 UTC on 5 November 2011 (a) with extreme and compound events, (b) with cyclone features and compound events. Rain, wind and wave extremes are denoted with blue, brown and green contours and shading; rain–wind compounds by slanted-line hatching, wave–wind compounds by square-grid hatching. Dry intrusions, cold fronts and warm conveyor belts are shown as yellow, aquamarine and purple objects, while thin red contours indicate the 500 and 1000 km radii around the centre and the thick red contour encircles the cyclone's impact area IA01 (definition in Section 3)

1. *cold front* masks intercepting a circle of 500 km radius from the cyclone centre;

2. *warm conveyor belt* masks intercepting a circle of 500 km radius from the cyclone centre;

3. *dry intrusion* masks intercepting a circle of 1000 km radius from the cyclone centre.

The interception criteria are satisfied when the concerned feature masks overlap in at least one grid point (see an example of IA01 for cyclone Rolf in Fig. 1).

In this work we prefer a large impact area definition (IA01) to a smaller definition based on a central area of 500 km radius (henceforth IA02) for three reasons: (i) IA01 allows the attribution of extreme winds and waves occurring at a considerable distance from the cyclone centre (Nissen et al., 2010; Pfahl, 2014; Field and Wood, 2007), (ii), in spite of being loose for the identification of cyclone-related precipitation extremes, IA01 captures distant rainfall events resulting from the interaction of the cyclonic flow with orography (Pfahl, 2014; Owen et al., 2021), and (iii) for comparability between rain–wind and wave–wind cyclone statistics. The differences between IA01 and IA02 are discussed in Appendix A. We also mention that the results using IA01 largely correspond to those using a fixed 1000 km radius impact area (not shown).

4 Frequencies of compound extremes and Mediterranean cyclones

The frequency of compound extremes is unevenly distributed across regions and seasons. Concomitant rain–wind extremes are most frequent in winter (Fig. 2) as a result of a winter peak in the uni-variate extremes (Fig. SM2) and in the compounding
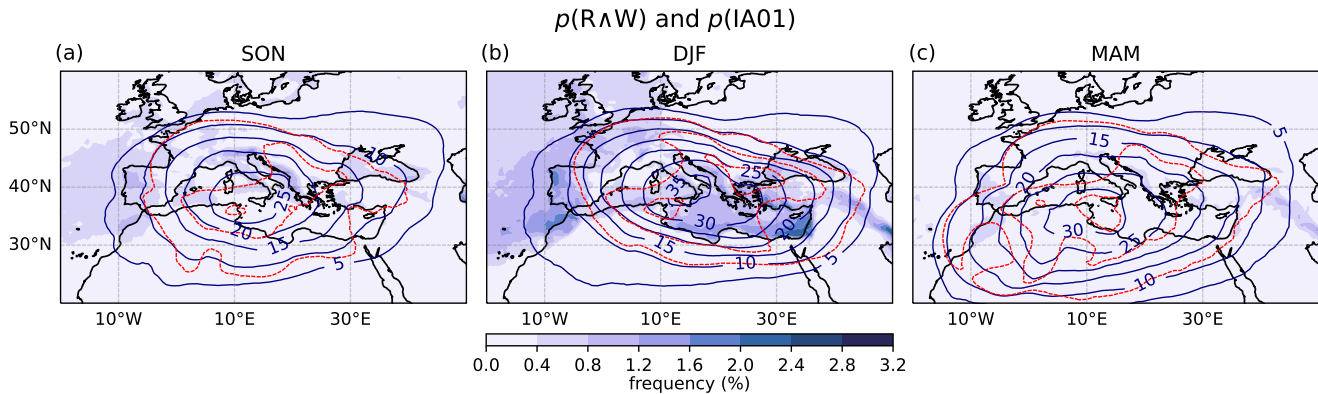
Figure 2. Frequency of R∧W compound (*p*(R∧W), shading) and of cyclone impact area (*p*(IA01), blue contours) in (a) autumn - SON, (b) winter - DJF and (c) spring - MAM. The frequency is expressed in percentage occurrence per time step for each season. The negative difference between *p*(IA02) and *p*(IA01) is represented by dashed red contours at 5% intervals
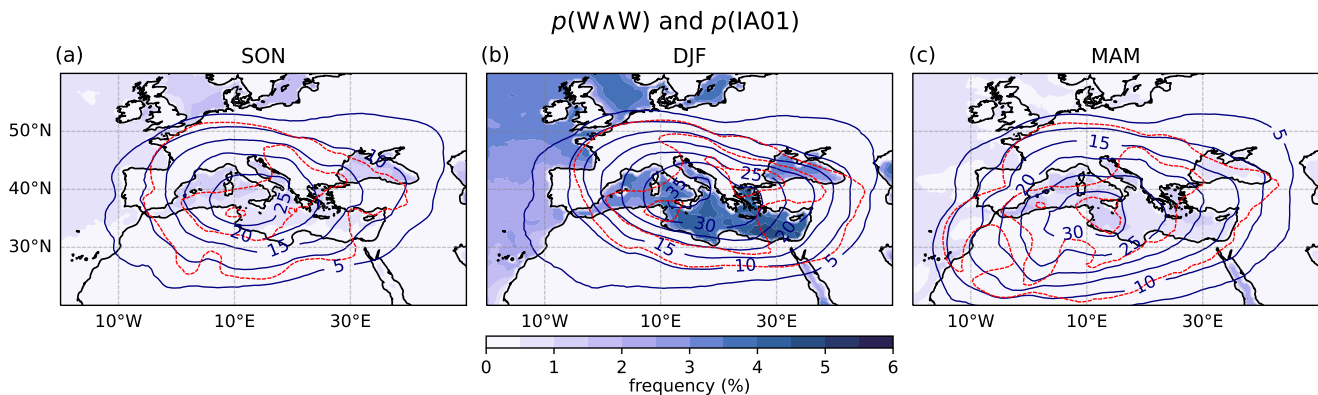
Figure 3. As in Fig. 2 for W∧W compound (note difference in colour scale)

ratio (*p*(R∧W)/*p*(R∨W), see Fig. SM5). The winter R∧W events occur most often in the eastern Mediterranean, specifically along the coastlines of Israel and North-Africa and of the eastern Adriatic sea. In agreement with Raveh-Rubin and Wernli (2015) (their Figs 3 and 4), the autumn spatial maximum in R∧W frequency is shifted to the central and western Mediterranean, where differences from the winter season are small. The spring frequency, limited by the number of extreme rainfall events (Fig. SM2(c)), is substantially lower everywhere (on average[9] about a half of the autumn and a quarter of the winter frequencies). The R∧W compounding ratio is generally highest over coastal regions facing north-west (Fig. SM5) and over orography (consistent with Fig. 2b in Owen et al. (2021) and Fig. 4a in Martius et al. (2016)).

Concomitant wave and wind extremes also occur most frequently in winter, but, differently from R∧W compounds, show a greater spatial homogeneity within the basin (Fig. 3). A shift in the position of the spatial maximum in compound frequency,

---

[9]Average over the Mediterranean region within 28°–50° N, 10° W–45° E, excluding white masked areas.

from the western Mediterranean in autumn to the eastern Mediterranean and the Black Sea in winter, is detected. Spring W∧W extremes display relatively small spatial variability with an average incidence similar to autumn values. The high compounding ratio across seasons (Fig. SM6) is a consequence of the strong physical dependence of wave height on the surface wind field (e.g., Komen et al., 1996). Nevertheless, both the frequency and the compounding ratio of W∧W events are generally higher in the Mediterranean than in the western Atlantic (cf. Fig. 1 in Catto and Dowdy, 2021).

The winter peak in compound extremes coincides with the highest frequency of cyclones (p(IA01), blue contours in Fig. 2). The Mediterranean cyclone density maximum shows a peak over the Italian peninsula in the autumn season, which expands towards the south east in winter and shifts towards the south west in spring (extending to northwestern Africa). The cyclone density distribution is spatially smoother and displays different regional and seasonal patterns compared with the compound frequency; factors such as geographical exposure and seasonal changes in the local climatological weather conditions account for the difference in the distribution of compound extremes.

4.1 Rain–wind compounds (R∧W)

The frequency of R∧W events within cyclones' impact areas (Fig. 4(a)-(c)) is highest in winter, with a 1 to 10% frequency over most of the basin, and lowest in spring - below 1% because of cyclones producing less rainfall (Flaounas et al., 2019).

The presence of a nearby cyclone increases the compound frequency (Fig. 4(d)-(f)), particularly in the transition seasons compared with winter and in the eastern and central Mediterranean, where a 10-fold amplification is not uncommon. The maps in Fig. 4(g)-(i), representing the proportion of cyclone-related R∧W compounds, show that autumn and spring events often co-occur with cyclones (on average[10] 50% and 58% of the R∧W events co-occur with cyclones in autumn and spring, compared with 48% in winter; differences are locally larger). Also, the association with cyclones is much stronger for R∧W compounds than for uni-variate extremes (cf. Fig. SM4). These results are not sensitive to the specific percentile threshold (cf. Fig. SM3, using the 95th percentile).

The relation between the quantities p(IA01| R∧W) and p(R∧W| IA01) in Fig. 4 follows Bayes' theorem (i.e., p(IA01| R∧W) $\cdot$ p(R∧W) = p(R∧W| IA01) $\cdot$ p(IA01)). The relation states that the fraction of cyclone-related compounds decreases with the ratio of cyclones over compounds, implying a smaller proportion of cyclone-related events in winter because of the distinct decline in p(IA01) / p(R∧W). The occurrence of winter R∧W events outside cyclones' impact areas is particularly high in the eastern and southern sectors of the Mediterranean (Fig. 4(h)), and coincides with where larger fractions of R∧W compounds co-occur with stray[11] dynamical features. This is shown in Fig. 5(b),(e), where unhatched areas indicate where less than 90% of the features occuring with compounds are related to a cyclone.

We next separate the influence of the Mediterranean cyclones' dynamical features, as in cold fronts (CF-IA), regions of warm conveyor belt inflow (WCBin-IA) and ascent (WCBas-IA), and dry intrusions (DI-IA), from the rest of the impact area (IA-noDF). Figure 6(a) shows the feature co-occurring most frequently with R∧W events, Figure 6(b) represents the feature maximising the R∧W event incidence; both are computed around the year because seasonal differences are small. Over the

---

[10]See footnote 9.

[11]The word "stray" is used to indicate features that do not fulfill the criteria for joining a Mediterranean cyclone's impact area, as described in Section 3.
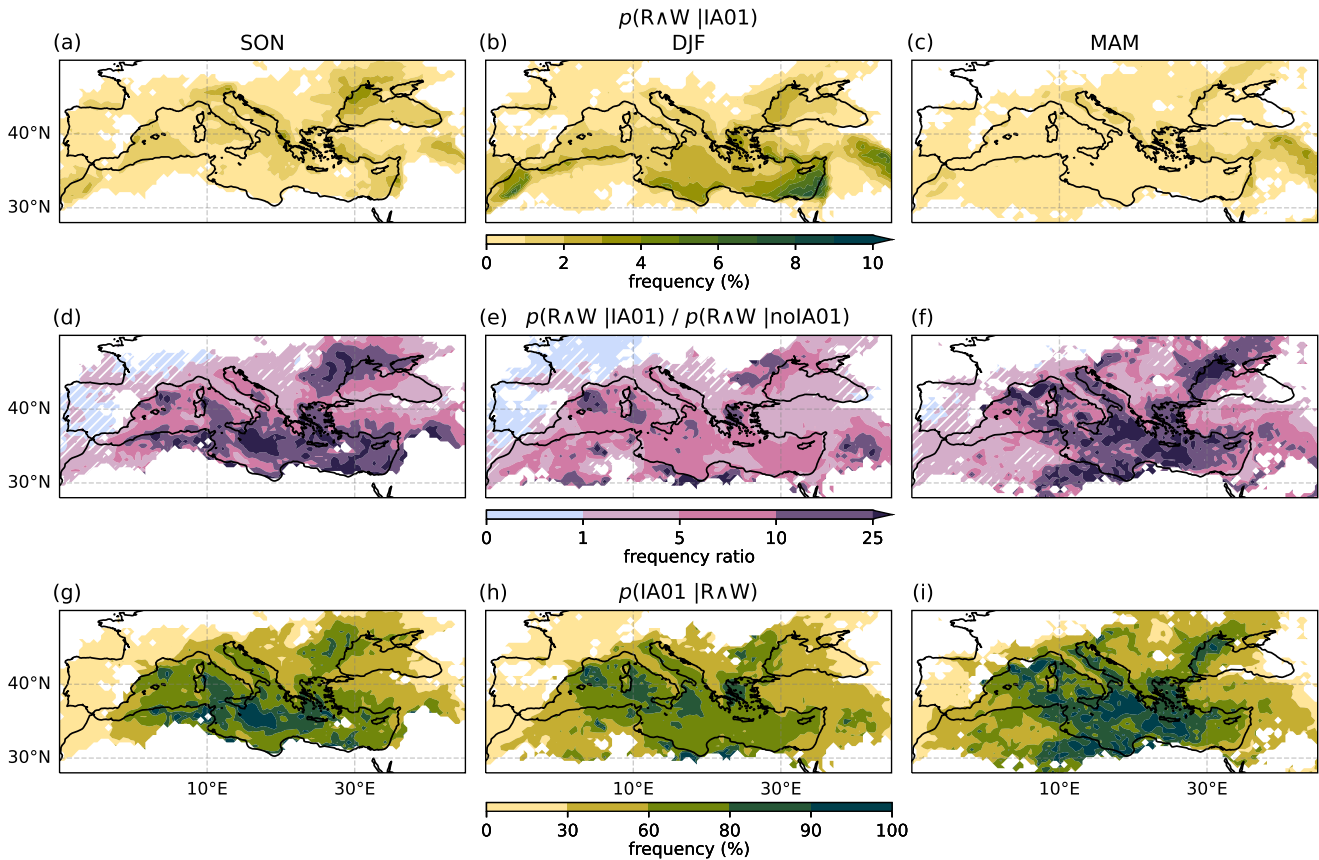
Figure 4. (a-c) The frequency of R∧W compound conditional to the presence of a cyclone, (d-f) the ratio of R∧W compound frequency during cyclone occurrence over the R∧W compound frequency during times when cyclones do not occur, (g-i) the cyclone frequency conditional to the presence of R∧W compounds. Results are shown by season (autumn - SON, winter - DJF, spring - MAM). In panels (d-f) the white slanted hatching indicates where compound frequency during cyclone occurrence is not significantly different from compound frequency during no-cyclone occurrence according to a two-sided z-test at 95% confidence level (Wilks, 2011). Grid points displaying less than four (R∧W |IA01) events are masked in white

whole Mediterranean region, the occurrence of R∧W events is maximised below the ascending branch of WCBs (Fig. 6(b)),
235   while the WCB inflow is more important over land and mountain reliefs during the winter season (not shown). On the other hand, when selecting the most frequent feature during R∧W compounds (Fig. 6(a)), WCB ascent is still predominant in the northern Mediterranean close to mountain reliefs or on sea-based grid points facing west- or south-oriented coasts (see also Fig. 7c for precipitation extremes in Pfahl et al., 2014). CFs show highest frequency on the rest of the basin (see also Fig. 4b for precipitation extremes in Catto and Pfahl, 2013), except around the North-African coasts, where the impact area without
240   dynamical features is relevant. The differences between panels (a) and (b) of Fig. 6 derive from the fact that in (b) the results are normalised by the features' individual frequencies (see Fig. SM7).
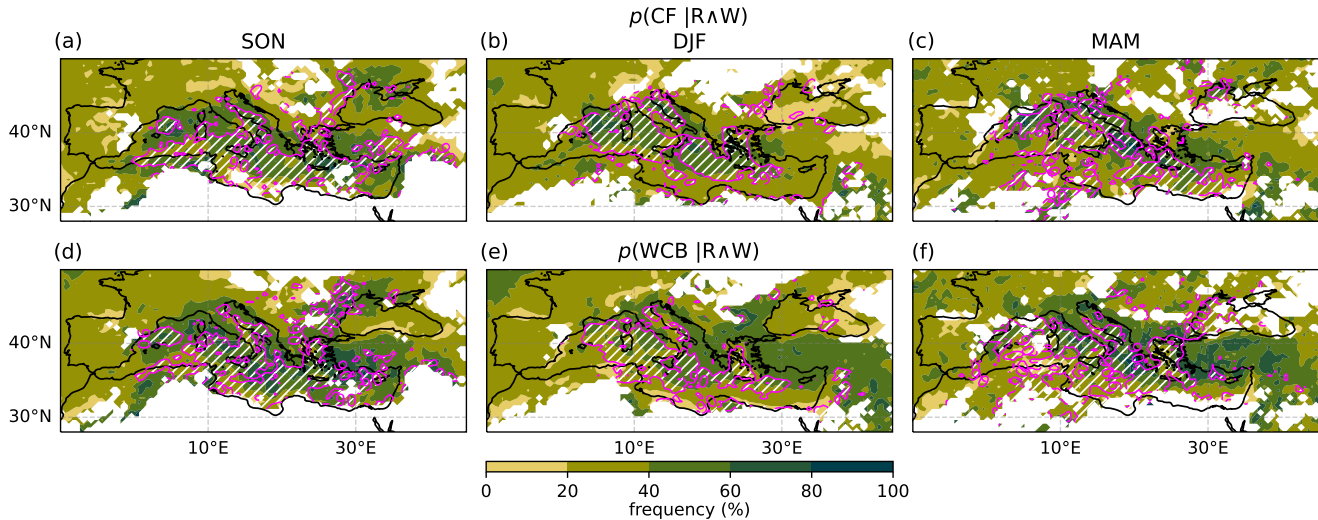
Figure 5. Frequency of (a-c) CFs and (d-f) WCBs conditional to R∧W compound occurrence in (a,d) autumn - SON, (b,e) winter - DJF and (c,f) spring - MAM. Note that in this plot we consider all CFs and WCBs, independently of their being part of a cyclone's impact area; magenta contours and slanted white hatching identify regions where more than 90% of the features are related to a cyclone (definition in Section 3). Note that, since compounds occurring within superposing CFs and WCBs contribute to the statistics of both, the sum of their conditional frequencies can exceed 100%

4.2 Wave–wind compounds (W∧W)

In the cyclone neighbourhood, wave–wind extremes occur much more frequently than rain–wind extremes (cf. Fig. 7(a)-(c) and Fig. 4(a)-(c)). The main similarity between the two types of compounds is the higher compound frequency for winter cyclones (in Fig. 7(b) W∧W reach and locally surpass a 10% frequency), and the tendency for the spatial peak in the cyclone compound density to shift from the western Mediterranean in autumn to the south-eastern basin in winter. This second aspect is coherent with the geographical shift in W∧W and impact area frequency (Fig. 3).

The proportion of W∧W events associated with cyclones peaks in the central part of the basin and is quite constant across seasons (on average[12] ∼50%, Fig. 7(g)-(i)). Moreover, the percentage of W∧W co-occurrence with cyclones, rarely exceeding an 80% level, is smaller compared with that of R∧W events (cf. Fig. 7(g)-(i) and 4(g)-(i)), and comparable to the rates computed for the uni-variate extremes (cf. Fig. SM4(c)-(i)). This suggests cyclones to be less relevant for W∧W than for R∧W compounding. The W∧W compound frequency increases approximately by a factor 5 in the cyclone neighbourhood (Fig. 7(d)-(f)), but exhibits a strong inter-seasonal variability which is likely related to a larger fraction of winter events occurring with stray dynamical features (Fig. SM9).

Dry intrusions, which drive intense surface wind gusts (Raveh-Rubin, 2017) and induce impacts on surface and atmospheric conditions (e.g., dust uplift, see Fluck and Raveh-Rubin, 2023), are the dynamical feature showing the highest frequency of

---

[12]See footnote 9.
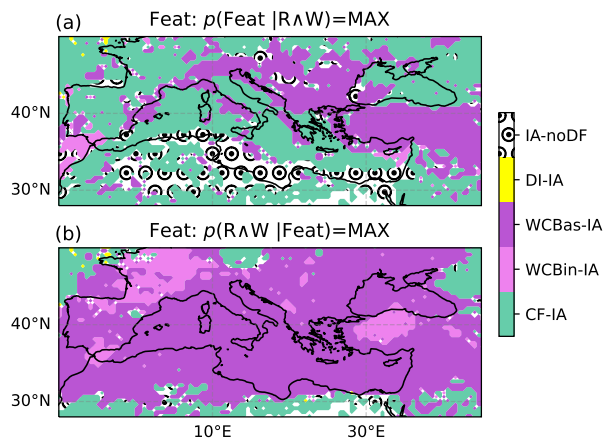
Figure 6. (a) The most frequent cyclone feature during R∧W compounds; (b) the cyclone feature associated with highest occurrence of R∧W compounds. We compute the conditional probability maxima amongst five cyclone features: the cold front (CF-IA), the warm conveyor belt inflow (WCBin-IA) and ascent (WCBas-IA) regions, the dry intrusion (DI-IA), and the 1000 km radius around the cyclone centre after removal of the aforementioned dynamical features' masks (IA-noDF). Compounds occurring within superposing CFs, WCBs and DIs contribute to the statistics of all the objects concerned. Because of a weak variability across seasons, the results are provided using year-round data

wave–wind compounding over the western and eastern parts of the basin (Fig. 8(b)). WCB ascent is important for W∧W in the central Mediterranean (comprising the Adriatic Sea and most of the Tirrenean and Ligurian Seas), south-east of Spain and in the eastern-most part of the basin. In contrast, CFs are the most frequent feature detected during W∧W events in the northern Mediterranean, replaced by the feature-free 1000 km radius in the southern Mediterranean (Fig. 8(a)).

4.3 Cyclone clusters relevant for compounding

In this section we refer to the Mediterranean cyclone clusters described in Givon et al. (2024a). While the association of each cluster with surface compounds from a cyclone centric view is discussed in Rousseau-Rizzi et al. (2023), here we show the cyclone clusters with the highest frequency of R∧W and W∧W from a (geographical) Eulerian perspective.

Baroclinic clusters 4 and 1 are, in order of importance, the most relevant for both types of compounds in autumn and winter (Figs 9 and 10). In winter we also find a strong regional association of cluster 8 with R∧W events over the western Mediterranean, and of cluster 5, typical of transition seasons, with both compound extremes in the central and south-eastern Mediterranean (the R∧W region in Fig. 9(e) is to the east of the W∧W region in Fig. 10(e), as expected in the schematic of Mediterranean cyclone impacts by Raveh-Rubin and Wernli (2016)). In autumn cluster 7, corresponding to daughter lows often originating over North Africa in a relatively dry environment, is important in the south-western Mediterranean and in the eastern-most part of the basin, but only relative to W∧W occurrence (Fig. 10(a),(d)).
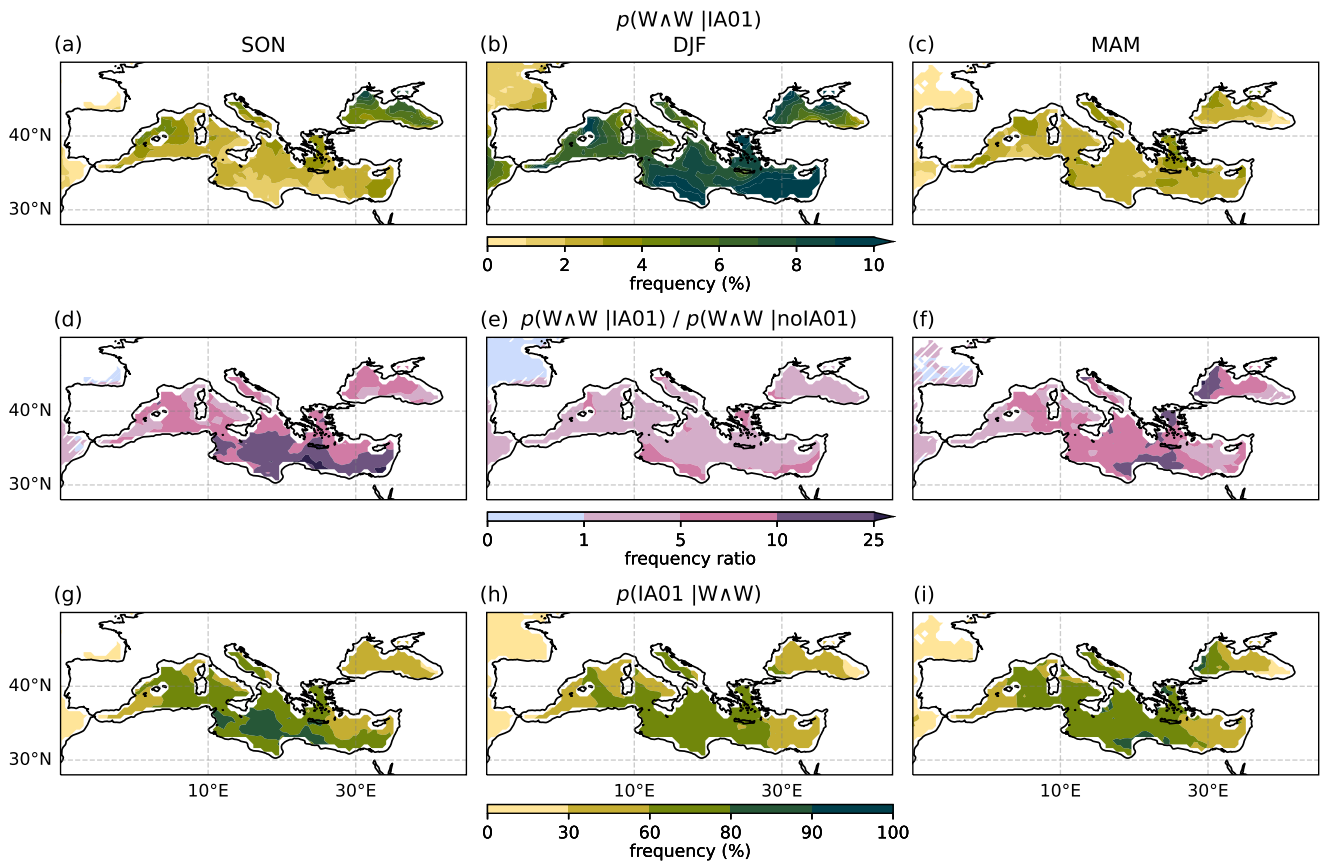
Figure 7. As in Fig. 4 for W∧W compound
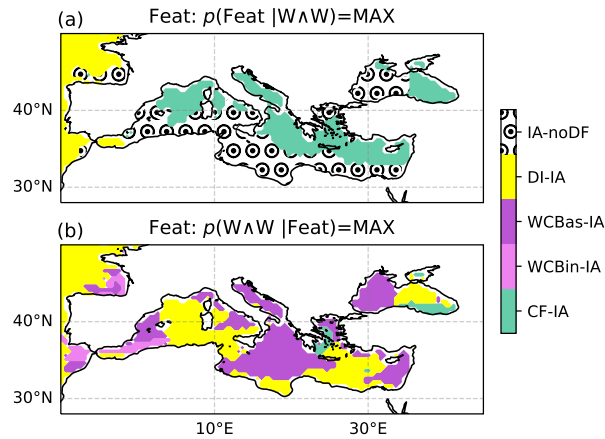
Figure 8. As in Fig. 6 for W∧W compound
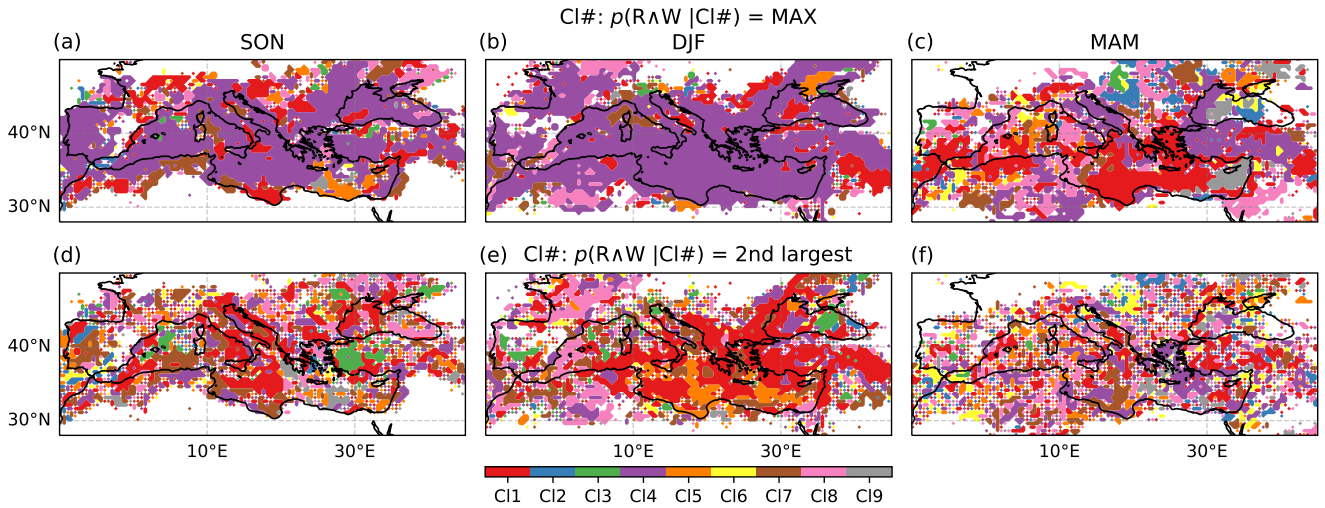
Figure 9. The first and second cyclone-cluster number (Cl#) maximising the R∧W compound frequency in (a,d) autumn - SON, (b,e) winter - DJF and (c,f) spring - MAM. Note that compounds occurring within multiple cyclones' IA01 contribute to the frequencies of all the relevant clusters. Note that grid points displaying less than four (R∧W |IA01) events are masked in white and that statistical noise results in irregular and intermittent colour patches
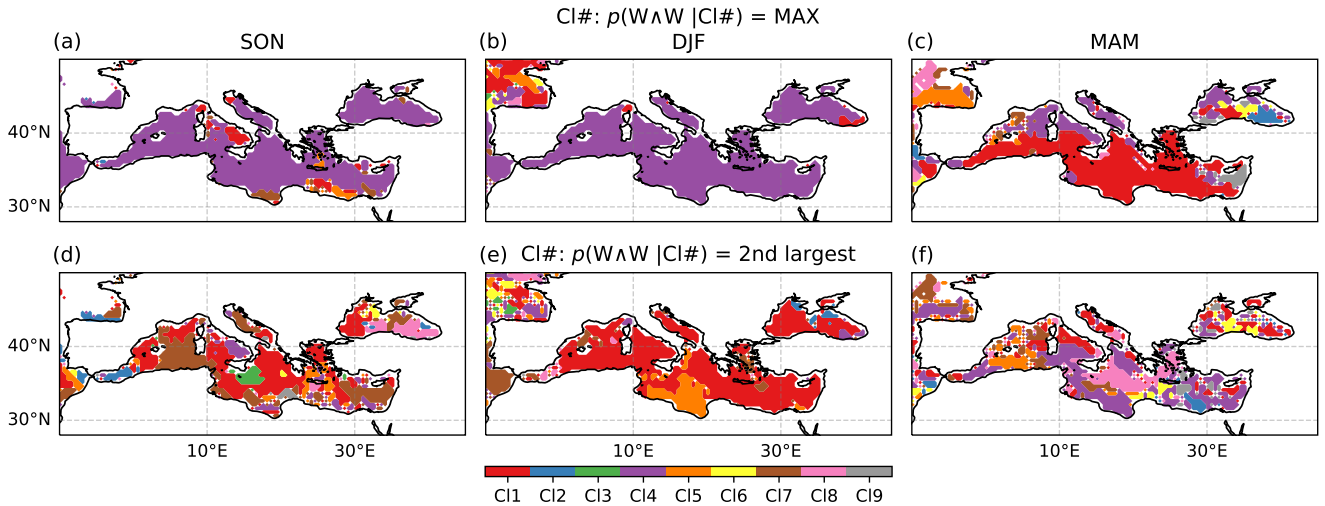
Figure 10. As in Fig. 9 for W∧W compound

In spring the dominant-cluster distribution is more diverse, with cluster 1 maximising the compound occurrence over most of the basin. Number 4, because of its frequency peaking earlier in winter, becomes the second most important cluster (first in the central-north Mediterranean). Cluster 9, corresponding to cut-off lows, acquires relevance for both types of compound in the eastern Mediterranean and in the Black Sea, while in the western Mediterranean the W∧W events are often linked to clusters 5

and 7, the R∧W events to the moister cluster 8. The sparse distribution of cluster 8 extends to a wide central Mediterranean region, where it is also associated with frequent W∧W events (Figs 9(c),(f) and 10(c),(f)). Cluster 2, typically comprising large, baroclinic winter cyclones, although identified by Rousseau-Rizzi et al. (2023) as the cluster with the highest simultaneity and overlap of rain and wind extremes, shows highest R∧W compound frequency only in spring over the Balkan peninsula. This is likely a result of its relatively low occurrence frequency compared with clusters 1 and 4 (Fig. SM8).

We note that clusters 1 and 4, dominant across regions and seasons, show an average R∧W and W∧W frequency that is only slightly higher than the aggregated statistics in Figs 4(a)-(c), 7(a)-(c), whereas summer clusters 6 and 9 and cluster 2, maximising compound frequency over limited domains, show an amplification of the overall cyclone compound frequency by a factor generally larger than 5. The other clusters, typical of the transition seasons, show an intermediate increase in R∧W and W∧W frequency (factors close to 3) compared with the aggregated statistics. Note that values are computed seasonally over the regions where each cluster maximises the compound probability, i.e., coulour-filled areas in Figs 9(a)-(c) and 10(a)-(c).

Table 1. List of cyclone clusters from Givon et al. (2024a) with synoptic setting, peak season and peak region of occurrence

Cluster No.	Synoptic Setting	Season	Region
1	stage-A lee low	winter	Ligurian Sea
2	anticyclonic, cyclonic wave-breaking low	winter	diverse
3	long-wave cutoff low	spring	Atlas mountains
4	stage-B lee low	winter	diverse
5	anticyclonic wave-breaking low	spring/autumn	Atlas mountains
6	heat low (Sharav)	summer	Sahara desert
7	daughter low	spring	diverse
8	cyclonic wave-breaking low	autumn	Ligurian sea
9	short-wave cutoff low	summer	diverse

5 Discussion

Frequency maps of rain–wind and wave–wind clustering show a pronounced winter peak and an eastward shift during the transition from autumn to spring (Fig. 2), following the density of the Mediterranean cyclones' impact area but with a more distinct seasonal cycle. Indeed, seasonal differences in compound frequencies are induced by climatological differences and by higher compounding around winter cyclones (Figs 4(a)-(c) and 7(a)-(c)), and only at a second order by the zcyclone frequency.

During the transition seasons compounds - R∧W in particular - happen mostly within the impact area of a cyclone (Figs 4(g)-(i) and 7(g)-(i)), while in winter they show a weaker relation to cyclones and happen more frequently with stray dynamical features (cf. Figs 4 and 5, Figs 7 and SM9). Moreover, the association with cyclones is stronger for R∧W extremes than for separate uni-variate extremes (cf. Fig. SM4). These results are consistent with Owen et al. (2021), who, with regard to winter R∧W compounds, highlight the importance of cold frontal regions far from storm centres and cite atmospheric rivers (ARs) as a potential driver (see also Hénin et al., 2021, for regional patterns). The high winter AR frequency in the region and

the associated potential increase in the likelihood of R∧W events support such hypothesis (Guan and Waliser, 2015; Waliser and Guan, 2017). Nevertheless, the association of ARs and rain–wind compounds around the Mediterranean basin and the superposition of AR and WCB objects (see discussion in Ralph et al., 2017) are yet to be systematically explored.

Geographical peculiarities, listed in the following, are more pronounced for R∧W compared with W∧W compounds, because of varying seasonal and regional moisture availability and of the strong effects of orography and coastlines on precipitation (e.g., Flaounas et al., 2019; Jansa et al., 2001; Pfahl, 2014). We also acknowledge that the statistical links between W∧W events and cyclones in the north-western Mediterranean basin (shown in Fig. 7) are sensitive to the inclusion of Atlantic cyclones, inducing strong wind impacts in the region (Pfahl, 2014; Nissen et al., 2010).

– The Gulf of Lion shows a year-round minimum in R∧W compounds-over-extremes ratio (Fig. SM5) and a maximum in the W∧W ratio (Fig. SM6). The rain–wind compounding ratio is related to dry northerly mistral-wind events that bear no rainfall yet are known to induce lee-cyclogenesis in the form of Genoa lows (Givon et al., 2024b). The systems thus formed carry intense precipitation elsewhere, mainly over the Italian and Balkan peninsulas (Givon et al., 2021). The maximum in W∧W compounding ratio is related to the high wind intensity in the region (Givon et al., 2024b, and the peak in the 98th percentile wind gust in Fig. SM1(e)) and to the physical dependence between the wave height and the wind field (e.g., Komen et al., 1996; Gentile et al., 2021).

– In Eastern Spain, south-western France and in the eastern alpine region a low proportion of R∧W events is associated (year-round) with Mediterranean cyclones (Fig. 4(g)-(i)). Despite the exclusion of Atlantic tracks, our results correspond qualitatively to those using global storm tracks by Owen et al. (2021), who relate the low co-occurrence of cyclones and R∧W compounds north of the Mediterranean (their Figs 10, 11, 12) to the fact that regional precipitation extremes are usually brought by Mediterranean cyclones, while wind extremes are often attributed to Atlantic weather systems. Similar findings are discussed in Pfahl (2014) and Nissen et al. (2010).

– The relation between cyclones and compounds is strong in the north west of the Black Sea (Fig. 4), because of a secondary peak in Mediterranean-cyclone-track density over the basin (see Fig. 13(b) in Flaounas et al. (2023)).

Regional differences in compound–cyclone statistics are further influenced by the varying size and type of the Mediterranean cyclones. For example, the high compound frequency around winter cyclones in the south eastern Mediterranean (Figs 4 and 7) can be attributed to the geographical exposure - the coast faces the north west, the direction from which most weather systems propagate (see also Fig. 4a in Martius et al., 2016), but also to the small size of cyclones favouring the superposition of wind and rain impacts close to the core of the system (see Fig 10 in Raveh-Rubin and Wernli, 2015). Our analyses confirm Raveh-Rubin and Wernli (2015)'s results by indicating a high ratio of compounds around eastern Mediterranean cyclones (Fig. 4(b)); this extends to the case when the impact area is restricted to a fixed 500 km radius (not shown).

Concerning the size of Mediterranean cyclones, we note that reducing the impact area extension (IA02 definition, see Section 3) does not determine qualitative changes in the results (cf. Figs 4, 7 and Figs A1, A2). However, further analyses in Appendix A demonstrate how the wider impact area IA01 is well suited for detecting cyclone-related wave–wind compounds

(c.f. Raveh-Rubin and Wernli, 2015, 2016), while the more stringent IA02 performs well in identifying cyclone-related rain–wind compounds. The suitability of IA02 for rain impacts partly verifies the attribution approach by Flaounas et al. (2018).

The Mediterranean cyclone clustering introduced in Givon et al. (2024a) allows us to study the spatial distribution of the cyclone types associated with highest compound frequency.

335 – Clusters 1 and 4, typically strong baroclinic cyclones, show the strongest connection with regional compounds across seasons, because of the high rainfall rates and of the wide wind footprints (Givon et al., 2024a; Rousseau-Rizzi et al., 2023). Their peak winter frequency helps to explain the maximum compound occurrence around winter cyclones (Fig. 4).

  – Cluster 8 cyclones, relatively stationary and characterised by strong convective activity, despite being associated with surface hazards of limited spatial extension (see Figs 5 and 11 in Givon et al. (2024a)), show a high likelihood of R∧W
340 compounds across multiple seasons and regions.

  – Cluster 5 and 7 cyclones are generated by the interaction of PV streamers with topography. Cluster 7 is relevant for W∧W extremes, cluster 5 for both compounds in winter, for W∧W in spring.

  – Cluster 9, i.e., cut-off lows typical of the extended summer season, emerges in spring over the eastern Mediterranean in connection with both types of compounds.

345 The results of the cluster analysis are independent of the specific definition of impact area (Section 3 and Appendix A).

Additionally, our study highlights the importance of cyclone-related dynamical features for the two types of compound extremes. The presence of WCB ascent maximises the likelihood of R∧W events across the Mediterranean region, although a frequency-weighed analysis suggests the importance of diverse air streams in the central and northern Mediterranean (CFs over the sea, WCBs over land and close to west- and south-facing coastal boundaries) and of the dynamical-feature-free impact
350 area along the southern Mediterranean coast (Fig. 6). The results for the southern coast are probably linked to a smaller size of the cyclones (Raveh-Rubin and Wernli, 2015) and to the presence of dry, weakly-precipitating WCBs from North Africa (Ziv et al., 2010). W∧W events are most likely below DIs and WCBs, although they co-occur frequently with CFs in the northern Mediterranean, and with the dynamical-feature-free impact area in the southern basin (Fig. 8). Results remain qualitatively unchanged when considering all dynamical features independently of their attribution to cyclone centres.

355 Although in literature the WCB is mainly connected to precipitation (Pfahl et al., 2014), in the Mediterranean region we find a high superposition of WCBs with rain–wind and wave–wind compounds (20-80% / 0-40% of the R∧W / W∧W events occur below a WCB, Fig. 5(d)-(f)). Regarding the plausibility of wind extremes below WCBs, a WCB jet in the form of strong geostrophic winds is not uncommon during the cyclone intensification stage in the Atlantic (Hewson and Neu 2015; Figs 7 and 9 in Eisenstein et al. 2023; Fig. 5 in Wernli 1997). Such "warm jet" usually starts in the lower troposphere ahead of the
360 cold front and ascends in the mid troposphere to the east of the cyclone centre. Convective activity embedded within the WCB (Flaounas et al., 2018), i.e., in pre-frontal environments (Catto et al., 2015; Pacey et al., 2023) or in regions of strong ascent near the cyclone centre (Flaounas et al., 2015), is known to induce downward momentum transport from the mid-troposphere thorough convective downdrafts (see discussion in Hewson and Neu, 2015), hence may favour the presence of strong surface

windgusts within the WCB. Wind channelling and forced ascent induced by coastal and orographic features (Carrera et al., 2009) combined with higher precipitation efficiency over land and orography (Flaounas et al., 2019; Pfahl, 2014; Houze Jr, 2012) may further contribute to the overlap of R∧W compounding and WCBs (cf. compound pattern and brown isohypse in Fig. 9 of Rousseau-Rizzi et al. (2023)).

6 Conclusions

We quantify the relation between compound weather extremes (rain–wind and wave–wind) and the presence of nearby cyclones in the extended Mediterranean region. Based on a new definition of "cyclone impact area", i.e., a fixed radius around the cyclone centre and overlapping fronts and cyclone air streams (Section 3), we answer the research questions listed in the Introduction.

1. We verify that the presence of a cyclone increases the odds of compound incidence, particularly in the transition seasons - by a factor 5 at least - and for R∧W events. Winter cyclones, even if less determinant for the occurrence of compound extremes, display the strongest compound frequency (1-10% for R∧W, more than 5% for W∧W). Differences between autumn and spring R∧W statistics are related to a lower moisture availability and to a southward extension of the storm track in the spring season. Additionally, R∧W extremes show a stronger link to cyclones than the two separate uni-variate extremes. (Section 4)

2. R∧W and W∧W compounding tend to overlap with different dynamical features around a cyclone, showing a distinct regional dependence. In general, the probability of rain–wind extremes around cyclones is maximised in areas of warm conveyor belt ascent (∼7% of the cases), that of wave–wind extremes below dry intrusion outflow and warm conveyor belts (more than 10% of the cases). Furthermore, in the northern Mediterranean region cold fronts are frequently detected during compound events, in the south it is the case of the feature-free cyclone impact area. (Sections 4.1, 4.2)

3. Baroclinic cyclones (clusters 1 and 4 from Givon et al. (2024a)) maximise the occurrence of compounds across all seasons, and their peak occurrence in winter explains the highest cyclone compound density for the winter season (see point 1.). Other cyclone categories are relevant at a local and seasonal scale. For example, compact, stationary and convective cyclones - classified as cluster 8 - are associated with frequent R∧W extremes over different seasons and parts of the basin. (Section 4.3)

Crucial questions remain regarding the role of orography and coastal boundaries, associated with wind channelling and forced ascent, in the generation of compound R∧W and W∧W events in the Mediterranean region. In particular, our results point to the importance of warm conveyor belts (WCBs) for rain–wind and wave–wind compounding in the northern Mediterranean, even though WCBs are principally known for rainfall impacts. Interactions of the WCBs with orography and coastal boundaries and WCB jet superposition with convective environments may be important for the generation of surface rain–wind extremes. Additionally, the role of atmospheric rivers, to be considered with potentially overlapping WCBs, in driving Mediterranean rain and rain–wind extremes deserves targeted analyses.

395   Future research could separate compounds in events induced by the synoptic circulation or by deep convection embedded around the cyclone. Based on previous literature (e.g., Flaounas et al., 2018; Givon et al., 2024a) we expect a different spatial extent and distribution (geographical and relative to the cyclone centre) of the two types of events. Additional insight on convective environments and hazards around Mediterranean cyclones will be addressed in a separate paper.

Finally, we expect Mediterrenean cyclone-related compounds in a future warmer climate to change in distribution and
400   intensity, following changes in the cyclones' frequency and physical properties. Recent trends show a decrease in the number of large baroclinic systems and an increase in the number of small cyclones typical of the extended summer season (Givon et al., 2024a). This agrees with end-of-XXI-century climate projections indicating a general reduction in the frequency and overall intensity of Mediterranean cyclones (Reale et al., 2022). In a warmer climate variations in the properties and surface impacts of cyclones are also expected (e.g., Manning et al., 2024, for cyclones over UK and Ireland). The connections of
405   Mediterranean cyclone changes with the regional distribution of compound extremes are yet to be examined.

Appendix A: Discussion on the choice of impact area

Various possibilities of impact areas were tested before establishing the definition of IA01 described in Section 3. Particularly interesting is the comparison between the results using IA01 and IA02, where the latter corresponds to a smaller central area (radius of 500 km instead of 1000 km) extended by the same dynamical features as IA01 (see Section 3). The frequency difference "$p(\text{IA02}) - p(\text{IA01})$" is shown in Fig. 2. Limit cases of IA01 and IA02 compound density correspond to:

i. all cyclone compounds (C) captured by IA01 fall within IA02

$p(C \,|\text{IA01-IA02}) = 0 \quad \Rightarrow \quad p(C \,|\text{IA02}) \gg p(C \,|\text{IA01})$ and $p(\text{IA02} \,|C) = p(\text{IA01} \,|C)$;

ii. the density of cyclone compounds is uniformly distributed within IA01

$p(C \,|\text{IA01}) = \text{const} \quad \Rightarrow \quad p(C \,|\text{IA02}) = p(C \,|\text{IA01})$ and $p(\text{IA02} \,|C) \ll p(\text{IA01} \,|C)$.

In (i.) the best choice is IA02, since IA01 overestimates the extension of the expected impacts and underestimates $p(C \,|\text{IA01})$, the compound occurrence around the cyclone; in (ii.) IA01 is most adequate, since IA02 underestimates the area of influence and $p(\text{IA02} \,|C)$, the ratio of cyclone-related compounds.
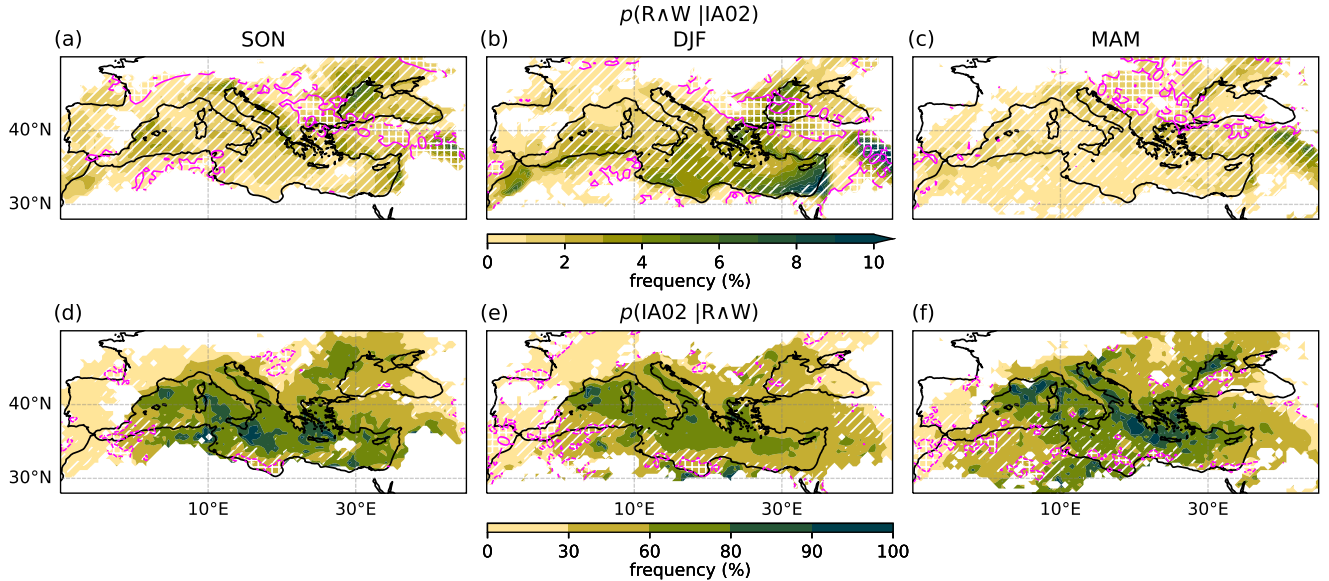
Figure A1. (a-c) The frequency of R∧W compound conditional to the presence of a cyclone, (d-f) the cyclone frequency conditional to the presence of R∧W compounds, using an impact area with a reference radius of 500 km (IA02). A difference between IA02 and IA01 frequencies by more than 25% of the IA01 value is denoted by white slanted-line hatching; a 50% difference is highlighted by white square-grid hatching within magenta contours (dashed for negative differences). Seasonal results for autumn - SON, winter - DJF and spring - MAM are displayed on the left, centre and right panels, respectively. Grid points displaying less than four (R∧W |IA02) events are masked out

In Fig. A1 we show in conditional probabilities between cyclones and R∧W compounds obtained using IA02, while hatching indicates percentage levels of difference from the same quantities computed using IA01 (full IA01 statistics in Fig. 4).

420 Differences between $p(R \wedge W \,|IA02)$ and $p(R \wedge W \,|IA01)$, positive and often exceeding the IA01 values by more than 25% (slanted-line hatching, panels (a)-(c) in Fig. A1), indicate a higher frequency of compounds within the smaller impact area. The largest differences in R∧W incidence are detected in the transition seasons, when cyclones are smaller and severe hazards are distributed closer to the cyclone centre (within IA02) (Givon et al., 2024a), and in the region separating the Mediterranean and the Black Sea. Hatching along the North-African coast in Fig. A1(d)-(f) also highlights a substantial regional decrease in

425 $p(IA02 \,|R \wedge W)$ relative to $p(IA01 \,|R \wedge W)$. This probably relates to IA02 missing distant compound events which result from the interaction between the large-scale cyclonic flow and the African topography.
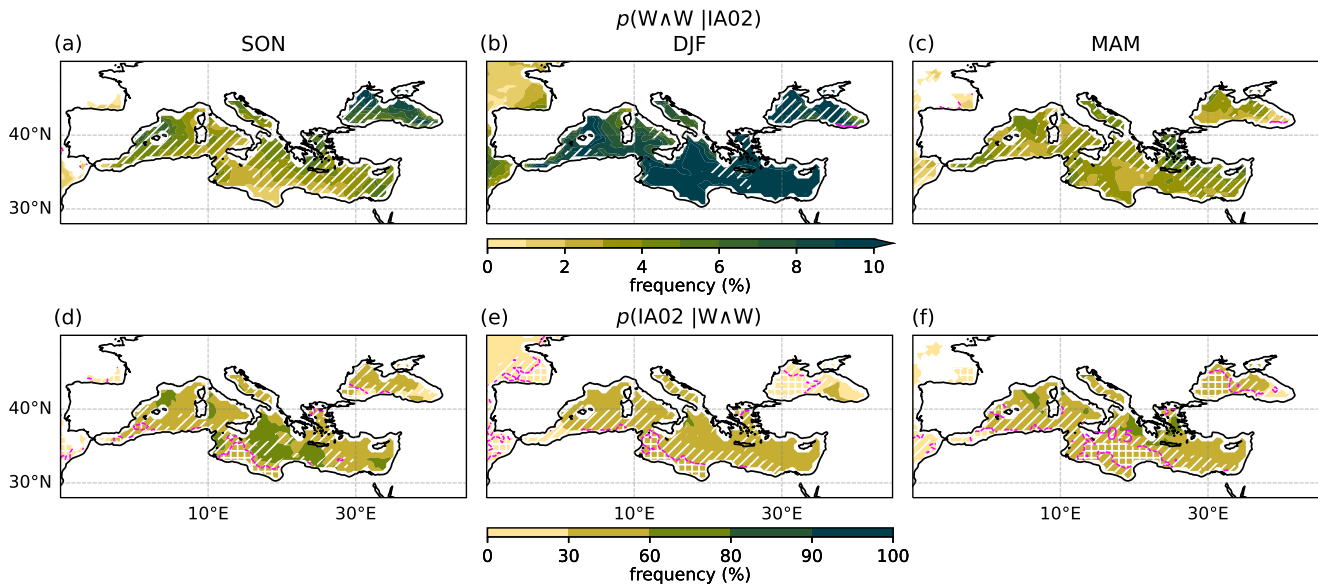
Figure A2. As in Fig. A1 for W∧W compound

The comparison of IA01 and IA02 for W∧W events diverges substantially from that of R∧W compounds (cf. Figs A2 and A1). The probability of W∧W within IA02 (Fig. A1(a)-(c)) does not increase nearly as much as in the case of R∧W, while the choice of IA02 strongly reduces the proportion of cyclone-related compounds throughout the Southern Mediterranean and

430 over the Black Sea (Fig. A1(d)-(f)).

In summary, rain–wind compounds, showing a large increase in compound frequency close to cyclones when using IA02, are reminiscent of limit-case (i.) with a preference for IA02 (except over the Southern Mediterranean coast). Differently, wave–wind compounds, because of small differences in the compound frequency within IA02 and IA01, and of an important fraction of compounds occurring outside IA02 but within IA01, are relatable to limit-case (ii.) and privilege IA01. This is consis-

435 tent with the expected geographical distribution of cyclone impacts, with intense rainfall and convective activity happening close to the centre, strong wind and waves occurring further away. The result validates previous hazard-dependent choices of Mediterranean-cyclone impact area (e.g., Flaounas et al., 2018); in this work, for the sake of methodological consistency across results, we use the IA01 definition.

Author contributions. AP, OM, SRR and JLC conceived the study. YG provided data and advise for the cyclone-cluster analysis. AP per-
formed the analyses and prepared the manuscript with contributions from all co-authors.

Competing interests. One of the authors is co-editor for Weather and Climate Dynamics.

Acknowledgements. AP is grateful for insightful discussions with Prof David Stephenson, Dr Matthew Priestley and Dr Emmanouil Flaounas,
and for the constructive contributions of the two reviewers. The authors are thankful to all the collaborators who produced and provided the
CF and DI datasets, and to Prof Heini Wernli and Prof Micheal Sprenger for kindly providing the WCB dataset. The research is funded by
the Swiss National Science Foundation (SNF) Grant Number IZCOZ0_205461, and contributes to the efforts of COST Action CA19109
"MedCyclones: European network for Mediterranean Cyclones in weather and climate". SRR acknowledges funding from the Israel Science
Foundation (grant number 1242/23) and the De Botton Center for Marine Science at the Weizmann Institute.

References

Bertotti, L. and Cavaleri, L.: The predictability of the" Voyager" accident, Natural Hazards and Earth System Sciences, 8, 533–537, 2008.

450 Čampa, J. and Wernli, H.: A PV perspective on the vertical structure of mature midlatitude cyclones in the Northern Hemisphere, Journal of the atmospheric sciences, 69, 725–740, 2012.

Campins, J., Genovés, A., Picornell, M., and Jansà, A.: Climatology of Mediterranean cyclones using the ERA-40 dataset, International Journal of Climatology, 31, 1596–1614, 2011.

Carlson, T. N.: Airflow through midlatitude cyclones and the comma cloud pattern, Monthly Weather Review, 108, 1498–1509, 1980.

455 Carrera, M. L., Gyakum, J. R., and Lin, C. A.: Observational study of wind channeling within the St. Lawrence River Valley, Journal of Applied Meteorology and Climatology, 48, 2341–2361, 2009.

Catto, J. L. and Dowdy, A.: Understanding compound hazards from a weather system perspective, Weather and Climate Extremes, 32, 100 313, 2021.

Catto, J. L. and Pfahl, S.: The importance of fronts for extreme precipitation, Journal of Geophysical Research: Atmospheres, 118, 10–791, 460 2013.

Catto, J. L. and Raveh-Rubin, S.: Climatology and dynamics of the link between dry intrusions and cold fronts during winter. Part I: global climatology, Climate Dynamics, 53, 1873–1892, 2019.

Catto, J. L., Madonna, E., Joos, H., Rudeva, I., and Simmonds, I.: Global relationship between fronts and warm conveyor belts and the impact on extreme precipitation, Journal of Climate, 28, 8411–8429, 2015.

465 Cavaleri, L., Bertotti, L., Torrisi, L., Bitner-Gregersen, E., Serio, M., and Onorato, M.: Rogue waves in crossing seas: The Louis Majesty accident, Journal of Geophysical Research: Oceans, 117, 2012.

Dafis, S., Rysman, J.-F., Claud, C., and Flaounas, E.: Remote sensing of deep convection within a tropical-like cyclone over the Mediterranean Sea, Atmospheric Science Letters, 19, e823, 2018.

De Luca, P., Messori, G., Pons, F. M., and Faranda, D.: Dynamical systems theory sheds new light on compound climate extremes in Europe 470 and Eastern North America, Quarterly Journal of the Royal Meteorological Society, 146, 1636–1650, 2020.

Dowdy, A. J. and Catto, J. L.: Extreme weather caused by concurrent cyclone, front and thunderstorm occurrences, Scientific Reports, 7, 40 359, 2017.

DWD: Selected Significant Events, https://www.dwd.de/EN/ourservices/rcccm/int/rcccm_int_sse.html?nn=495490&cl2Categories_Jahr= 2011&cl2Categories_Monat=rcccm_int_sse_11&cl2Categories_LeistungsId=rcccm_int_sse&lsId=446082, [Online; accessed 9-April-475 2024], 2011.

Eisenstein, L., Schulz, B., Pinto, J. G., and Knippertz, P.: Identification of high-wind features within extratropical cyclones using a probabilistic random forest – Part 2: Climatology over Europe, Weather and Climate Dynamics, 4, 981–999, https://doi.org/10.5194/wcd-4-981-2023, 2023.

Fanti, V., Ferreira, Ó., Kümmerer, V., and Loureiro, C.: Improved estimates of extreme wave conditions in coastal areas from calibrated 480 global reanalyses, Communications Earth & Environment, 4, 151, 2023.

Field, P. R. and Wood, R.: Precipitation and cloud structure in midlatitude cyclones, Journal of climate, 20, 233–254, 2007.

Flaounas, E., Raveh-Rubin, S., Wernli, H., Drobinski, P., and Bastin, S.: The dynamical structure of intense Mediterranean cyclones, Climate Dynamics, 44, 2411–2427, 2015.

Flaounas, E., Kotroni, V., Lagouvardos, K., Gray, S. L., Rysman, J.-F., and Claud, C.: Heavy rainfall in Mediterranean cyclones. Part I: contribution of deep convection and warm conveyor belt, Climate dynamics, 50, 2935–2949, 2018.

Flaounas, E., Fita, L., Lagouvardos, K., and Kotroni, V.: Heavy rainfall in Mediterranean cyclones, Part II: Water budget, precipitation efficiency and remote water sources, Climate Dynamics, 53, 2539–2555, 2019.

Flaounas, E., Davolio, S., Raveh-Rubin, S., Pantillon, F., Miglietta, M. M., Gaertner, M. A., Hatzaki, M., Homar, V., Khodayar, S., Korres, G., et al.: Mediterranean cyclones: Current knowledge and open questions on dynamics, prediction, climatology and impacts, Weather and Climate Dynamics, 3, 173–208, 2022.

Flaounas, E., Aragão, L., Bernini, L., Dafis, S., Doiteau, B., Flocas, H., L. Gray, S., Karwat, A., Kouroutzoglou, J., Lionello, P., et al.: A composite approach to produce reference datasets for extratropical cyclone tracks: Application to Mediterranean cyclones, Weather and Climate Dynamics Discussions, 2023, 1–32, 2023.

Fluck, E. and Raveh-Rubin, S.: Dry air intrusions link Rossby wave breaking to large-scale dust storms in Northwest Africa: Four extreme cases, Atmospheric Research, 286, 106 663, 2023.

Froidevaux, P., Schwanbeck, J., Weingartner, R., Chevalier, C., and Martius, O.: Flood triggering in Switzerland: the role of daily to monthly preceding precipitation, Hydrology and Earth System Sciences, 19, 3903–3924, 2015.

Gentile, E. S., Gray, S. L., Barlow, J. F., Lewis, H. W., and Edwards, J. M.: The impact of atmosphere–ocean–wave coupling on the near-surface wind speed in forecasts of extratropical cyclones, Boundary-Layer Meteorology, 180, 105–129, 2021.

Givon, Y., Keller Jr, D., Silverman, V., Pennel, R., Drobinski, P., and Raveh-Rubin, S.: Large-scale drivers of the mistral wind: link to Rossby wave life cycles and seasonal variability, Weather and Climate Dynamics, 2, 609–630, 2021.

Givon, Y., Hess, O., Flaounas, E., Catto, J. L., Sprenger, M., and Raveh-Rubin, S.: Process-based classification of Mediterranean cyclones using potential vorticity, Weather and Climate Dynamics, 5, 133–162, https://doi.org/10.5194/wcd-5-133-2024, 2024a.

Givon, Y., Keller Jr, D., Pennel, R., Drobinski, P., and Raveh-Rubin, S.: Decomposing the role of dry intrusions for ocean evaporation during mistral, Quarterly Journal of the Royal Meteorological Society, 2024b.

Guan, B. and Waliser, D. E.: Detection of atmospheric rivers: Evaluation and application of an algorithm for global studies, Journal of Geophysical Research: Atmospheres, 120, 12 514–12 535, 2015.

Gutiérrez-Fernández, J., Miglietta, M. M., González-Alemán, J. J., and Gaertner, M. A.: A new refinement of Mediterranean tropical-like cyclones characteristics, Geophysical Research Letters, 51, e2023GL106 429, 2024.

Guzzetti, F., Peruccacci, S., Rossi, M., and Stark, C. P.: The rainfall intensity–duration control of shallow landslides and debris flows: an update, Landslides, 5, 3–17, 2008.

Heitmann, K., Sprenger, M., Binder, H., Wernli, H., and Joos, H.: Warm conveyor belt characteristics and impacts along the life cycle of extratropical cyclones: Case studies and climatological analysis based on ERA5, EGUsphere, 2023, 1–42, 2023.

Hénin, R., Ramos, A. M., Pinto, J. G., and Liberato, M. L.: A ranking of concurrent precipitation and wind events for the Iberian Peninsula, International Journal of Climatology, 41, 1421–1437, 2021.

Hepworth, E., Messori, G., and Vichi, M.: Association between extreme atmospheric anomalies over Antarctic sea ice, Southern Ocean polar cyclones and atmospheric rivers, Journal of Geophysical Research: Atmospheres, 127, e2021JD036 121, 2022.

Hersbach, H., Bell, B., Berrisford, P., Hirahara, S., Horányi, A., Muñoz-Sabater, J., Nicolas, J., Peubey, C., Radu, R., Schepers, D., et al.: The ERA5 global reanalysis, Quarterly Journal of the Royal Meteorological Society, 146, 1999–2049, 2020.

Hewson, T. D.: Objective fronts, Meteorological Applications, 5, 37–65, 1998.

Hewson, T. D. and Neu, U.: Cyclones, windstorms and the IMILAST project, Tellus A: Dynamic Meteorology and Oceanography, 67, 27 128, 2015.

Houze Jr, R. A.: Orographic effects on precipitating clouds, Reviews of Geophysics, 50, 2012.

Impact Forecasting LLC: November 2011 Monthly Cat Recap, https://web.archive.org/web/20181202193349/http://thoughtleadership. aonbenfield.com/documents/201112_if_monthly_cat_recap_november.pdf, [Online; accessed 12-January-2024], 2011.

Jansa, A., Genoves, A., Picornell, M. A., Campins, J., Riosalido, R., and Carretero, O.: Western Mediterranean cyclones and heavy rain. Part 2: Statistical approach, Meteorological Applications, 8, 43–56, 2001.

Kilsdonk, R. A., Bomers, A., and Wijnberg, K. M.: Predicting Urban Flooding Due to Extreme Precipitation Using a Long Short-Term Memory Neural Network, Hydrology, 9, 105, 2022.

Klawa, M. and Ulbrich, U.: A model for the estimation of storm losses and the identification of severe winter storms in Germany, Natural Hazards and Earth System Sciences, 3, 725–732, 2003.

Komen, G. J., Cavaleri, L., Donelan, M., Hasselmann, K., Hasselmann, S., and Janssen, P.: Dynamics and modelling of ocean waves, 1996.

Lavers, D. A., Simmons, A., Vamborg, F., and Rodwell, M. J.: An evaluation of ERA5 precipitation for climate monitoring, Quarterly Journal of the Royal Meteorological Society, 148, 3152–3165, 2022.

Lionello, P., Trigo, I. F., Gil, V., Liberato, M. L., Nissen, K. M., Pinto, J. G., Raible, C. C., Reale, M., Tanzarella, A., Trigo, R. M., et al.: Objective climatology of cyclones in the Mediterranean region: a consensus view among methods with different system identification and tracking criteria, Tellus A: Dynamic Meteorology and Oceanography, 68, 29 391, 2016.

Madonna, E., Wernli, H., Joos, H., and Martius, O.: Warm conveyor belts in the ERA-Interim dataset (1979–2010). Part I: Climatology and potential vorticity evolution, Journal of climate, 27, 3–26, 2014.

Manning, C., Kendon, E. J., Fowler, H. J., Catto, J. L., Chan, S. C., Sansom, P. G., et al.: Compound wind and rainfall extremes: Drivers and future changes over the UK and Ireland, Weather and Climate Extremes, p. 100673, 2024.

Martius, O., Pfahl, S., and Chevalier, C.: A global quantification of compound precipitation and wind extremes, Geophysical Research Letters, 43, 7709–7717, 2016.

Minola, L., Zhang, F., Azorin-Molina, C., Pirooz, A. S., Flay, R., Hersbach, H., and Chen, D.: Near-surface mean and gust wind speeds in ERA5 across Sweden: towards an improved gust parametrization, Climate Dynamics, 55, 887–907, 2020.

Nissen, K., Leckebusch, G., Pinto, J. G., Renggli, D., Ulbrich, S., and Ulbrich, U.: Cyclones causing wind storms in the Mediterranean: characteristics, trends and links to large-scale patterns, Natural Hazards and Earth System Sciences, 10, 1379–1391, 2010.

Obermann-Hellhund, A.: State of the Simulation of Mesoscale Winds in the Mediterranean and Opportunities for Improvements, Atmosphere, 13, 1007, 2022.

Owen, L. E., Catto, J. L., Stephenson, D. B., and Dunstone, N. J.: Compound precipitation and wind extremes over Europe and their relationship to extratropical cyclones, Weather and Climate Extremes, 33, 100 342, 2021.

Pacey, G., Pfahl, S., Schielicke, L., and Wapler, K.: The climatology and nature of warm-season convective cells in cold-frontal environments over Germany, Natural Hazards and Earth System Sciences Discussions, 2023, 1–28, 2023.

Papritz, L., Pfahl, S., Rudeva, I., Simmonds, I., Sodemann, H., and Wernli, H.: The role of extratropical cyclones and fronts for Southern Ocean freshwater fluxes, Journal of Climate, 27, 6205–6224, 2014.

Pfahl, S.: Characterising the relationship between weather extremes in Europe and synoptic circulation features, Natural Hazards and Earth System Sciences, 14, 1461–1475, 2014.

Pfahl, S. and Wernli, H.: Quantifying the relevance of cyclones for precipitation extremes, Journal of Climate, 25, 6770–6780, 2012.

Pfahl, S., Madonna, E., Boettcher, M., Joos, H., and Wernli, H.: Warm conveyor belts in the ERA-Interim dataset (1979–2010). Part II: Moisture origin and relevance for precipitation, Journal of Climate, 27, 27–40, 2014.

Ralph, F. M., Dettinger, M., Lavers, D., Gorodetskaya, I. V., Martin, A., Viale, M., White, A. B., Oakley, N., Rutz, J., Spackman, J. R., et al.: Atmospheric rivers emerge as a global science and applications focus, Bulletin of the American Meteorological Society, 98, 1969–1973, 2017.

Raveh-Rubin, S.: Dry intrusions: Lagrangian climatology and dynamical impact on the planetary boundary layer, Journal of Climate, 30, 6661–6682, 2017.

Raveh-Rubin, S. and Wernli, H.: Large-scale wind and precipitation extremes in the Mediterranean: a climatological analysis for 1979–2012, Quarterly Journal of the Royal Meteorological Society, 141, 2404–2417, 2015.

Raveh-Rubin, S. and Wernli, H.: Large-scale wind and precipitation extremes in the Mediterranean: dynamical aspects of five selected cyclone events, Quarterly Journal of the Royal Meteorological Society, 142, 3097–3114, 2016.

Reale, M., Cabos Narvaez, W. D., Cavicchia, L., Conte, D., Coppola, E., Flaounas, E., Giorgi, F., Gualdi, S., Hochman, A., Li, L., et al.: Future projections of Mediterranean cyclone characteristics using the Med-CORDEX ensemble of coupled regional climate system models, Climate dynamics, pp. 1–24, 2022.

Ridder, N. N., Pitman, A. J., Westra, S., Ukkola, A., Do, H. X., Bador, M., Hirsch, A. L., Evans, J. P., Di Luca, A., and Zscheischler, J.: Global hotspots for the occurrence of compound events, Nature communications, 11, 5956, 2020.

Rivoire, P., Martius, O., and Naveau, P.: A comparison of moderate and extreme ERA-5 daily precipitation with two observational data sets, Earth and Space Science, 8, e2020EA001 633, 2021.

Rousseau-Rizzi, R., Raveh-Rubin, S., Catto, J., Portal, A., Givon, Y., and Martius, O.: A storm-relative climatology of compound hazards in Mediterranean cyclones, EGUsphere, 2023, 1–31, 2023.

Sansom, P. G. and Catto, J. L.: Improved objective identification of meteorological fronts: a case study with ERA-Interim, Geoscientific Model Development Discussions, pp. 1–19, 2022.

Schultz, D. M.: Reexamining the cold conveyor belt, Monthly Weather Review, 129, 2205–2225, 2001.

Schultz, D. M., Bosart, L. F., Colle, B. A., Davies, H. C., Dearden, C., Keyser, D., Martius, O., Roebber, P. J., Steenburgh, W. J., Volkert, H., et al.: Extratropical cyclones: A century of research on meteorology's centerpiece, Meteorological monographs, 59, 16–1, 2019.

Seneviratne, S. I., Nicholls, N., Easterling, D., Goodess, C. M., Kanae, S., Kossin, J., Luo, Y., Marengo, J., McInnes, K., Rahimi, M., and et al.: Changes in Climate Extremes and their Impacts on the Natural Physical Environment, p. 109–230, Cambridge University Press, 2012.

Sprenger, M., Fragkoulidis, G., Binder, H., Croci-Maspoli, M., Graf, P., Grams, C. M., Knippertz, P., Madonna, E., Schemm, S., Škerlak, B., et al.: Global climatologies of Eulerian and Lagrangian flow features based on ERA-Interim, Bulletin of the American Meteorological Society, 98, 1739–1748, 2017.

The Washington Post: Mediterranean storm brings heavy rain and flooding to Italy and France, https://www.washingtonpost.com/blogs/capital-weather-gang/post/mediterranean-storm-brings-heavy-rain-and-flooding-to-italy-and-france/2011/11/09/gIQAim3N5M_blog.html, [Online; accessed 9-April-2024], 2011.

Trigo, I. F.: Climatology and interannual variability of storm-tracks in the Euro-Atlantic sector: a comparison between ERA-40 and NCEP/NCAR reanalyses, Climate Dynamics, 26, 127–143, 2006.

Trigo, I. F., Davies, T. D., and Bigg, G. R.: Objective climatology of cyclones in the Mediterranean region, Journal of climate, 12, 1685–1696, 1999.

Utsumi, N., Kim, H., Kanae, S., and Oki, T.: Which weather systems are projected to cause future changes in mean and extreme precipitation in CMIP5 simulations?, Journal of Geophysical Research: Atmospheres, 121, 10–522, 2016.

Waliser, D. and Guan, B.: Extreme winds and precipitation during landfall of atmospheric rivers, Nature Geoscience, 10, 179–183, 2017.

600 Wernli, H.: A Lagrangian-based analysis of extratropical cyclones. II: A detailed case-study, Quarterly Journal of the Royal Meteorological Society, 123, 1677–1706, 1997.

Wernli, H. and Davies, H. C.: A Lagrangian-based analysis of extratropical cyclones. I: The method and some applications, Quarterly Journal of the Royal Meteorological Society, 123, 467–489, 1997.

Wilks, D. S.: Statistical methods in the atmospheric sciences, vol. 100, Academic press, 2011.

605 Zhang, Z. and Li, X.-M.: Global ship accidents and ocean swell-related sea states, Natural Hazards and Earth System Sciences, 17, 2041–2051, 2017.

Ziv, B., Saaroni, H., Romem, M., Heifetz, E., Harnik, N., and Baharad, A.: Analysis of conveyor belts in winter Mediterranean cyclones, Theoretical and applied climatology, 99, 441–455, 2010.

Zscheischler, J., Westra, S., Van Den Hurk, B. J., Seneviratne, S. I., Ward, P. J., Pitman, A., AghaKouchak, A., Bresch, D. N., Leonard, M.,
610 Wahl, T., et al.: Future climate risk from compound events, Nature Climate Change, 8, 469–477, 2018.

Zscheischler, J., Martius, O., Westra, S., Bevacqua, E., Raymond, C., Horton, R. M., van den Hurk, B., AghaKouchak, A., Jézéquel, A., Mahecha, M. D., et al.: A typology of compound weather and climate events, Nature reviews earth & environment, 1, 333–347, 2020.